ACCSCIENCE PUBLISHING

OR

ORIGINAL RESEARCH ARTICLE

Self-organizing vascularized subchondral bone organoids from stromal vascular fraction enable functional osteochondral interface regeneration

Supplementary Files

1. Quantification of collagen fiber diameter and density

Quantitative analysis of collagen fibers was performed using ImageJ software. For each sample, five non-overlapping transmission electron microscopic images were analyzed. The fiber diameter was measured by manually tracing the minor axis of individual collagen fibrils. At least 30 fibrils were measured per group to ensure statistical significance.

Collagen fiber density was defined as the number of fibrils per μm^2 of extracellular matrix (ECM) area. The ECM area was delineated manually to exclude cellular components. All measurements were conducted by two independent, blinded investigators.

Data were expressed as mean ± standard deviation (SD). Statistical comparisons between the control (AM) and subchondral bone organoid (SSBO) groups were conducted using an unpaired two-tailed Student's *t*-test, with $p<0.05$ considered statistically significant.

2. Immunofluorescence and quantification of vascular networks

Tissue sections were stained with mouse anti-human CD31 antibody (1:100, ab9498, Abcam, UK) and rat anti-mouse CD31 antibody (1:100, ab222783, Abcam, UK) to visualize endothelial structures. After incubation with a fluorescent secondary antibody and 4',6-diamidino-2-phenylindole nuclear counterstaining, images were captured using a multispectral imaging system (MSP-REM-P1E-Vectra Polaris, Akova Biosciences, USA).

Quantitative analysis of vascular morphology was performed using AngioTool software (Version 0.6a, National Cancer Institute, United States of America). Parameters, including the total number of junctions and total vessel branch length, were calculated from binarized CD31-stained images. For each sample, 3–5 random high-power fields (HPFs) were analyzed. Results were expressed as mean ± SD, and statistical differences between AM and SSBO groups were assessed using an unpaired Student's *t*-test.

3. Immunohistochemical quantification of osteocalcin (OCN) and osterix (OSX) expression

For immunohistochemical analysis, paraffin-embedded tissue sections from subcutaneous implants (for OCN) and osteochondral defect sites (for OSX) were deparaffinized, rehydrated, and subjected to antigen retrieval using citrate buffer (pH 6.0). Endogenous peroxidase activity was blocked with 3% hydrogen peroxide, followed by incubation with primary antibodies against OCN (1:200; ab93876, Abcam, UK) and OSX (1:200; ab209484, Abcam, UK) overnight at 4°C.

After incubation with horseradish peroxidase-conjugated secondary antibodies and 3,3'-diaminobenzidine chromogen development, sections were counterstained with hematoxylin. Images were captured using a bright-field microscope (BX53, Olympus, Japan).

Quantitative analysis was performed using ImageJ software. The percentage of positively stained area relative to the total tissue area was calculated from 3 randomly selected HPFs per sample. Data were expressed as mean ± SD, and statistical comparisons between groups were conducted using an unpaired Student's *t*-test.

4. Histological evaluation of cartilage repair

Cartilage repair at the defect site was assessed using hematoxylin and eosin, Safranin O, and Masson's trichrome staining. Histological scoring was performed using the O'Driscoll scoring system, which evaluates parameters including cellular morphology, matrix staining, surface regularity, and cartilage thickness. Scoring was conducted independently and by two blinded investigators. The total O'Driscoll score was used to compare the quality of cartilage regeneration between groups.

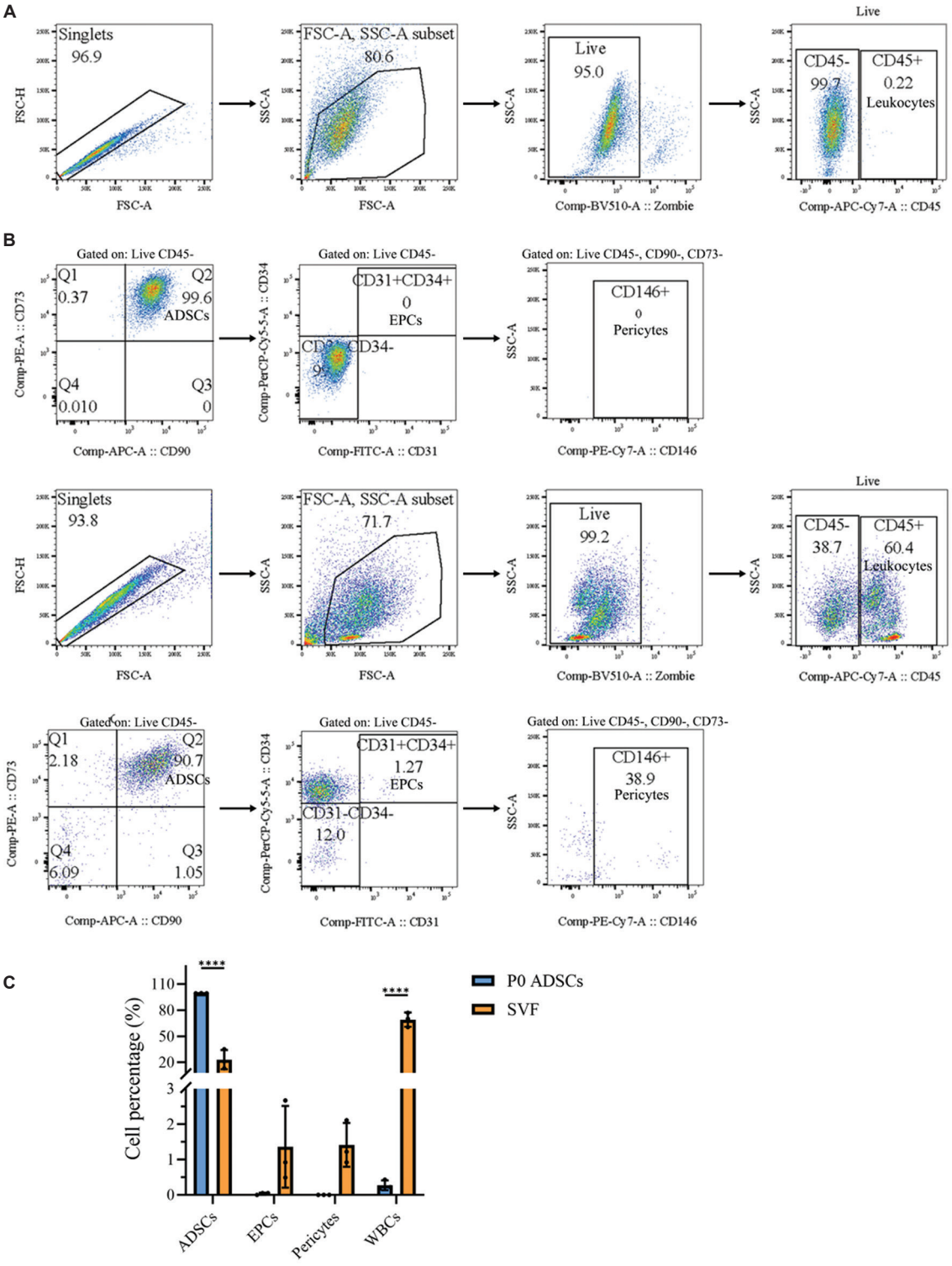

Figure S1. Flow cytometry gating strategy for P0 ADSCs and SVF. P0 ADSCs (A) and SVF (B) were gated by FSC-A versus FSC-H to exclude debris and doublets, followed by the selection of viable cells based on live/dead staining. CD45 expression was used to separate $CD45^+$ leukocytes from $CD45^-$ stromal cells. Within the $CD45^-$ population, ADSCs were defined as $CD90^+CD73^+$, EPCs as $CD34^+CD31^+$, and pericytes as $CD146^+CD90^-CD73^-$. $CD45^+$cells were collectively defined as leukocytes (WBCs). (C) Quantitative flow cytometric analysis of P0 ADSCs and SVF.

Note: ****$p<0.0001$.

Abbreviations: ADSCs: Adipose-derived stem cells; CD: Cluster of differentiation; EPCs: Endothelial progenitor cells; FSC-A: Forward scatter area; FSC-H: Forward scatter height; P0: Primary; SSBO: Subchondral bone organoid; SSC-A: Side scatter area; SVF: Stromal vascular fraction; WBCs: White blood cells.

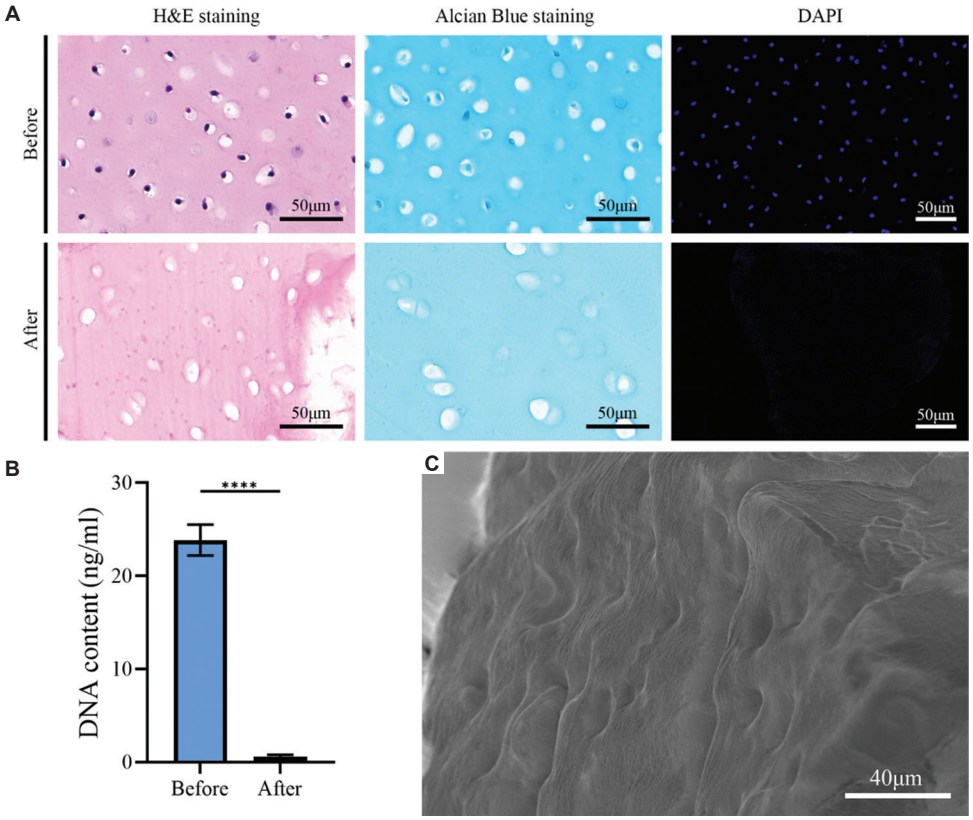

Figure S2. Characterization of dECM microparticles. (A) Representative images of cartilage stained with H&E, Alcian Blue, and DAPI, illustrating structural and cellular changes before and after decellularization. Scale bar: 50 μm; magnification: 30.5×. (B) Quantitative analysis of residual DNA content in cartilage extracellular matrix. (C) Scanning electron microscopic image of dECM microparticles. Scale bar: 50 μm; magnification: 2×.
Note: ****$p<0.0001$.
Abbreviations: DAPI: 4',6-diamidino-2-phenylindole; dECM: Decellularized extracellular matrix; H&E: Hematoxylin and eosin.

Table S1. Primer sequences, including forward and reverse primers

Gene	Forward primers	Reverse primers
SOX9	5'-GACTTCCGCGACGTGGAC-3'	5'-CAGTACCTGCCGCCCAAC-3'
COL2A1	5'-GGCAATAGCAGGTTCACGTACA-3'	5'-CGATAACAGTCTTGCCCCACTT-3'
COL10A1	5'-CTAGTGGACTCCCTTCAGGAAC-3'	5'-CGCTAAGCTCAGTCACTCCAG-3'
COL1A1	5'-TCCAACGAGATCGAGATCC-3'	5'-AAGCCGAATTCCTGGTCT-3'
RUNX2	5'-GTGATAAATTCAGAAGGGAGG-3'	5'-CTTTTGCTAATGCTTCGTGT-3'
VEGF	5'-AGGAGGAGGGCAGAATCATCA-3'	5'-CTCGATTGGATGGCAGTAGCT-3'
CD31	5'-GACGTGCTCTTTTACAACATCTC-3'	5'-CCTCACGATCCCACCTTGG-3'
OCN	5'-AGCCACCGAGACACCATGAGA-3'	5'-CTCCTGAAAGCCGATGTGGTC-3'
GAPDH	5'-TGACGCTGGGGCTGGCATTG-3'	5'-GGCTGGTGGTCCAGGGGTCT-3'
IL1B	5'-GGACAGGATATGGAGCAACAAGTGG-3'	5'-TCATCTTTCAACACGCAGGACAGG-3'
IL10	5'-GTGATGCCCCAAGCTGAGA-3'	5'-CACGGCCTTGCTCTTGTTTT-3'

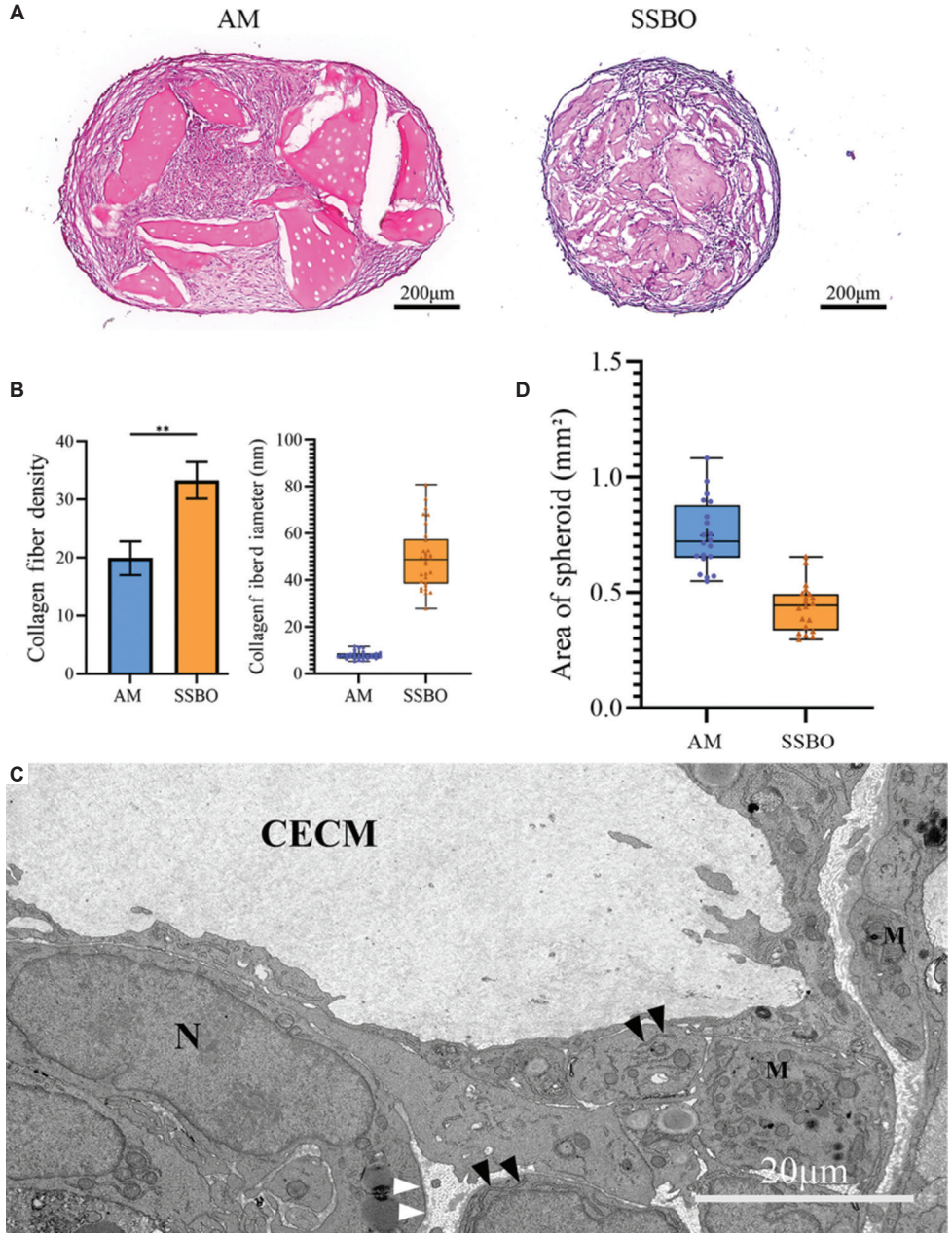

Figure S3. Comparative morphological and ultrastructural analysis of SSBO and AM spheroids after 14 days of three-dimensional culture. (A) Hematoxylin and eosin staining on SSBO and AM spheroids after 14 days of three-dimensional culture. Scale bar: 200 μm; magnification: 8×. (B) Quantitative analysis of collagen fiber ultrastructure. (C) Transmission electron microscopic images of the SSBO group after 14 days of culture. Black arrowheads indicate the endoplasmic reticulum. White arrowheads point to collagen fibers. "N" marks the nucleus, and "M" marks the mitochondria. Scale bar: 20 μm; magnification: 3×. (D) Spheroid diameters after 14 days of culture, revealing differences in size between SSBO and AM.

Abbreviations: AM: Control group (adipose-derived stem cells with cartilage extracellular matrix); CECM: Cartilage extracellular matrix; SSBO: Subchondral bone organoid.

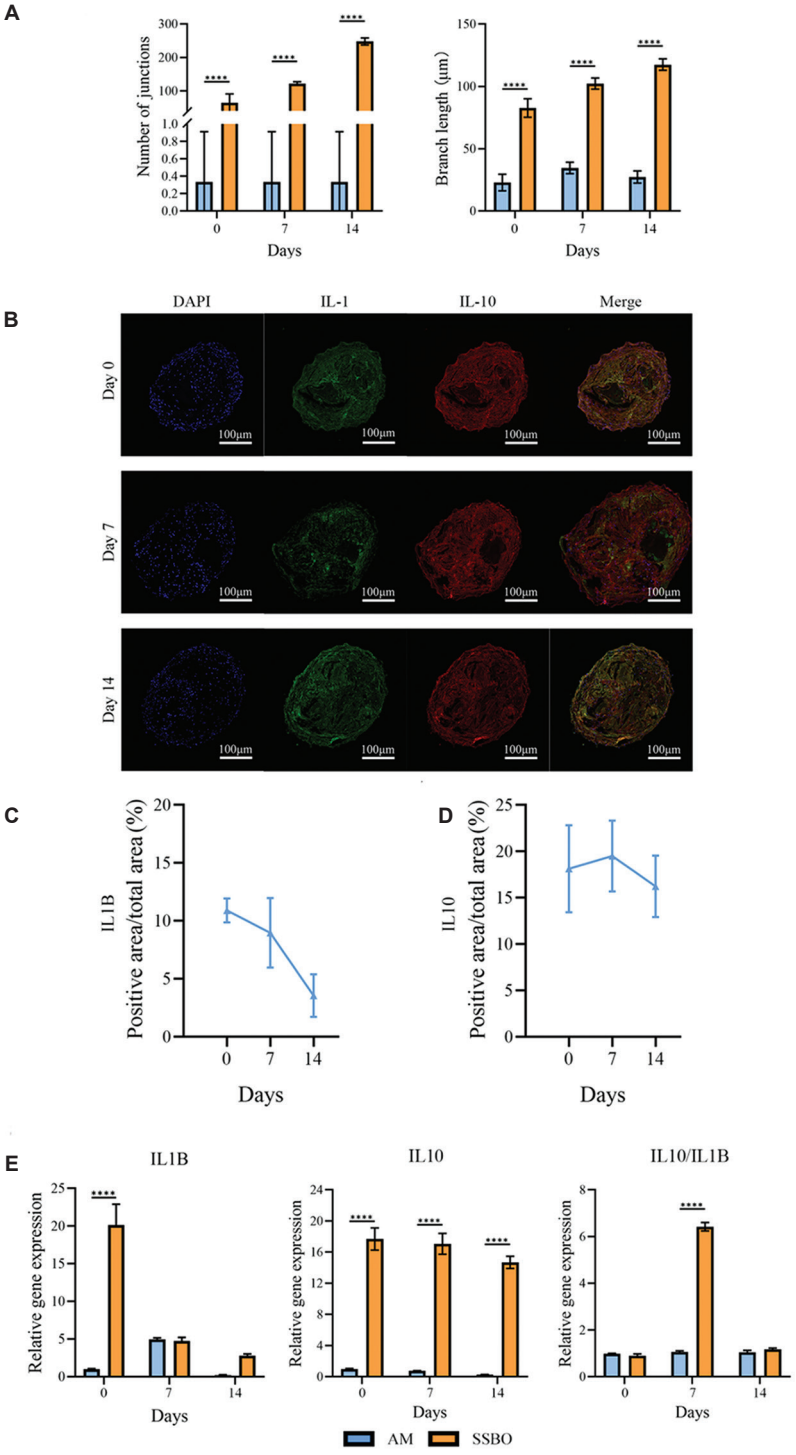

Figure S4. Temporal analysis of inflammatory marker expression and vascular structure in SSBO and AM spheroids during three-dimensional culture. (A) Quantification of total junctions and branch length. (B) Representative multicolor immunofluorescence images of SSBO and AM on days 0, 7, and 14 of culture. From left to right: Nuclear staining (DAPI), IL-1β, IL-10, and merged images (Merge). Scale bar: 100 μm; magnification: 10×. (C) and (D) Quantification of the positive staining area (%) for IL-1β and IL-10. (E) Quantitative polymerase chain reaction analysis of IL-1β and IL-10 markers in both groups. Gene expression levels were normalized to the AM group at day 0.

Notes: ****p<0.0001; All data are presented as mean ± standard deviation (n = 3/group).

Abbreviations: AM: Control group (adipose-derived stem cells with cartilage extracellular matrix); DAPI: 4',6-diamidino-2-phenylindole; IL: Interleukin; SSBO: Subchondral bone organoid.

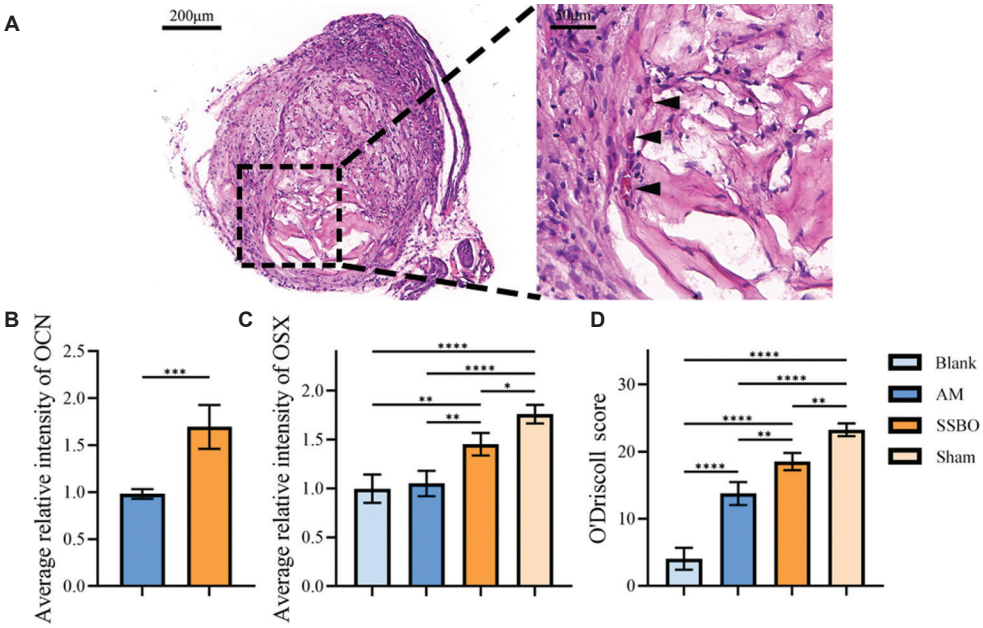

Figure S5. Histological and immunohistochemical evaluation of bone and cartilage regeneration in subcutaneous and defect models. (A) Hematoxylin and eosin staining on regenerated tissues harvested 3 weeks after subcutaneous implantation in nude mice, showing histological differences between groups. Scale bars: 50 μm, 200 μm; magnifications: 20×, 8×. (B) Quantitative analysis of OCN immunohistochemical staining in subcutaneous implants in nude mice. (C) Quantitative analysis of OSX immunohistochemical staining in regenerated tissue at the defect site. (D) Histological evaluation of cartilage repair using O'Driscoll scoring system.

Notes: Statistical significance: *p<0.05; **p<0.01; ***p<0.001; ****p<0.0001. All data are presented as mean ± standard deviation (n = 3/group).

Abbreviations: AM: Control group (adipose-derived stem cells with cartilage extracellular matrix); OCN: Osteocalcin; OSX: Osterix; SSBO: Subchondral bone organoid.